Optimal Control Policies for Tubular Reactors Experiencing Catalyst Decay: II. Multiple-Bed Semiregenerative Reactors

A. F. OGUNYE and W. H. RAY
University of Waterloo, Waterloo, Ontario, Canada

The optimal control problem for multiple beds is formulated and a distributed maximum principle derived. Gradient methods are then used to synthesize the optimal control policies for some examples in three-bed isothermal and adiabatic reactors. Finally, examples are worked to illustrate the computational algorithm in adiabatic beds when optimal catalyst loading is to be determined, and when it is desired to distribute the feed in an optimal fashion between the beds. Reasonably good convergence was obtained in all the examples, so that the method appears quite feasible for determining optimal control policies in multiple reactors subject to catalyst decay.

The optimal control of single-bed tubular reactors subject to catalyst decay has been treated in reference *1*,* and an effective computational algorithm based on a distributed maximum principle demonstrated. However, many of the commercial processes cited in I are commonly carried out in multiple-bed reactors with interstage heating or cooling for better reaction temperature control and interstage feed distribution to provide better selectivity or yield control. Owing to the significance of this type of process, we shall extend the theory and computational algorithms of I to the case of multiple beds operated in a semiregenerative manner.†

First we shall define the multiple-bed reactor optimization problem clearly and extend the maximum principle developed in I to cover this case. Then we shall work out in detail examples to demonstrate both the generality of the algorithm and the efficiency of the gradient method when applied to multiple beds.

THE MULTIPLE-BED REACTOR

In modeling our multiple-bed reactor we shall assume the total length to be L' with a finite number of discontinuities α_k which represent the points of separation between the beds. If we assume that at any discontinuity k we are free to add component i, then q'_{ik} represents the feed rate of component i added at discontinuity α_k. In this case the rate of change of component i due to reaction in reactor k is

$$\frac{\partial \xi_i}{\partial z'} = \left\{ \sum_{l=1}^{r} \sum_{j=1}^{k} q'_{lj} \right\}^{-1} f_i'(\boldsymbol{\xi}, \boldsymbol{\Psi}, T, P) \quad \begin{matrix} 0 \leq z' \leq L' \\ 0 \leq t' \leq \theta \end{matrix} \tag{1}$$

$$i = 1, 2, \ldots\ldots r \qquad k = 1, 2, \ldots\ldots N + 1$$

$$\xi_i(\alpha_k{}^+, t') = h_i(q'_{lj}, \xi_m(\alpha_k{}^-, t')) \tag{2}$$

where Equation (1) shows the effect of increasing by interstage feeds the total material reacting, and Equation (2) is a blending equation which determines the feed to the next section of reactor. Note that we have allowed a feed q_{iN+1} after the N^{th} reactor. This was done to allow for the possibility that bypassing some of the feed may be optimal, for example, when the blending Equation (2) is highly nonlinear. In a similar way we may write equations for temperature and pressure variations in the spatial direction.

As in I we shall assume that the change of the j^{th} catalyst activity at any point is given by

$$\frac{\partial \psi_j}{\partial t'} = g_j'(\xi_i, \psi_k, T, P) \quad 0 \leq z' \leq L', \quad 0 \leq t' \leq \theta \tag{3}$$

where the initial catalyst activity may be set as

$$\psi_j(z', 0) = \psi_{j0}(z') \tag{4}$$

These equations can be put in the form

$$\frac{\partial x_i}{\partial z} = f_i(\mathbf{x}, \mathbf{y}, \mathbf{u}_k, \mathbf{q}_k) \quad \begin{matrix} 0 \leq z \leq 1 \\ 0 \leq t \leq 1 \end{matrix} \quad i = 1, 2, \ldots r \tag{5}$$

$$x_i(\alpha_k{}^+, t) = h_i(\mathbf{q}_l, x_j(\alpha_k{}^-, t)) \qquad k = 1, 2, \ldots N + 1 \tag{6}$$

where Equation (5) is most general form of Equation (1). Similarly Equations (3) and (4) can be generalized to

$$\frac{\partial y_j}{\partial t} = g_j(\mathbf{x}, \mathbf{y}, \mathbf{u}_k) \quad 0 \leq z \leq 1, \quad 0 \leq t \leq 1 \tag{7}$$

$$y_j(z, 0) = w_j(z) \qquad j = 1, 2, \ldots q \tag{8}$$

where both spatial and temporal directions have been normalized. The reactor configuration is shown in Figure 1. The state variables now are **x** and **y** and our controls are interior controls in the k^{th} bed $\mathbf{u}_k$ (temperatures, etc.), catalyst loading **w**, and feed at k^{th} bed $\mathbf{q}_k$. Now that we have described the multiple-bed model, let us develop a maximum principle for solving the optimization problem.

THE OPTIMIZATION PROBLEM

The optimization problem is as stated in Equation (7) of I, where we assume that the optimal run time can be determined separately by a univariate search on θ. Thus our problem is to determine the control policy (for a fixed value of θ) which maximizes the objective functional

$$I = \int_0^1 G_1(x_i(1, t), \mathbf{q}_l)dt + \int_0^1 G_2(y_j(z, 1), w_j)dz$$

A. F. Ogunye is at the University of Ife, Ile-Ife, Nigeria. W. H. Ray is at the State University of New York, Buffalo, New York.

* Henceforth denoted as I.

† A semiregenerative mode of operation is one in which all reactors are shut down and regenerated at once at the end of the catalyst life.

$$+ \int_0^1 \int_0^1 G(\mathbf{x}, \mathbf{y}, \mathbf{u}_k, \mathbf{q}_l)\,dz\,dt \qquad (9)$$

where G_1 accounts for the value of product concentrations, heat credits for exit temperatures, feed costs, etc.; G_2 accounts for catalyst cost, salvage value of the spent catalyst, etc.; and G accounts for heating and cooling costs, etc. The maximization of Equation (9) is subject to constraint Equations (5) to (8) being satisfied as well as upper and lower bounds on the control variables. In order to provide a theory for such problems we shall provide a weak maximum principle.

Theorem

In order for the controls $\mathbf{u}_k$, $\mathbf{w}$, $\mathbf{q}_l$ to be optimal controls for the problem given by Equations (5) to (9), it is necessary for all unconstrained $\mathbf{u}_k(z, t)$ that*

$$\frac{\partial H}{\partial \mathbf{u}_k} = \frac{\partial G}{\partial \mathbf{u}_k} + \lambda_i \frac{\partial f_i}{\partial \mathbf{u}_k} + \mu_j \frac{\partial g_j}{\partial \mathbf{u}_k} \qquad (10)$$

vanish almost everywhere on $0 \leqq z \leqq 1$, $0 \leqq t \leqq 1$, and

$$H = G + \lambda_i f_i + \mu_j g_j \qquad (11)$$

to be a maximum with respect to $\mathbf{u}_k(z, t)$ at constraints. For $\mathbf{u}_k(z)$ the conditions

$$\int_0^1 \frac{\partial H}{\partial \mathbf{u}_k}\,dt = 0 \qquad (12)$$

for unconstrained $\mathbf{u}_k(z)$ and $\int_0^1 H dt$ being a maximum for constrained $\mathbf{u}_k(z)$ must hold. Similarly for $\mathbf{u}_k(t)$ the conditions

$$\int_0^1 \frac{\partial H}{\partial \mathbf{u}_k}\,dz = 0 \qquad (13)$$

for unconstrained $\mathbf{u}_k(t)$ and $\int_0^1 H dz$ being a maximum with respect to constrained $\mathbf{u}_k(t)$ must hold.

In addition, for $\mathbf{q}_l$ to be optimal it is necessary that

$$\frac{\partial H_1}{\partial \mathbf{q}_l} = \int_0^1 \left[\frac{\partial G}{\partial \mathbf{q}_l} + \lambda_i \frac{\partial f_i}{\partial \mathbf{q}_l}\right] dz + \frac{\partial G_1}{\partial \mathbf{q}_l} + \sum_{k=1}^{N} \lambda_i(\alpha_k^+, t)\,\frac{\partial h_i}{\partial \mathbf{q}_l} = 0 \qquad (14)$$

for unconstrained $\mathbf{q}_l$ and

$$H_1 = G_1 + \int_0^1 [G + \lambda_i f_i]dz + \sum_{k=1}^{N} \lambda_i(\alpha_k^+, t) h_i \{\mathbf{q}_j, x_j(\alpha_k^-, t)\} \qquad (15)$$

be a maximum with respect to constrained $\mathbf{q}_l$. For the case where $\mathbf{q}_l$ is independent of t, the conditions $\int_0^1 \frac{\partial H_1}{\partial \mathbf{q}_l}\,dt = 0$ and $\int_0^1 H_1\,dt$ a maximum must hold for unconstrained and constrained $\mathbf{q}_l$, respectively.

Finally, for $w_j(z)$ to be optimal, it is necessary that

$$\frac{\partial H_2}{\partial w_j} = \frac{\partial G_2}{\partial w_j} + \mu_j(z, 0) = 0 \qquad (16)$$

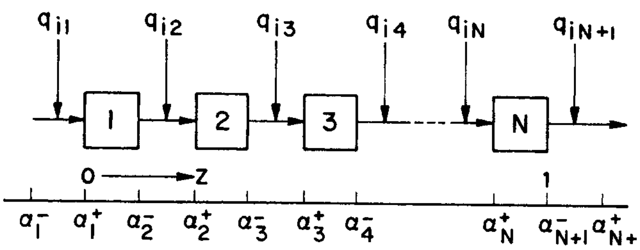

Fig. 1. The multiple-bed reactor system.

for unconstrained w_j and

$$H_2 = G_2 + \mu_j(z, 0) w_j(z) \qquad (17)$$

be a maximum with respect to constrained $w_j(z)$. For the case where w_j is independent of z, the conditions $\int_0^1 \frac{\partial H_2}{\partial w_j}\,dz = 0$ and $\int_0^1 H_2\,dz$ a maximum must hold for unconstrained and constrained w_j, respectively.

The adjoint variables are defined by

$$\frac{\partial \lambda_i}{\partial z} = \frac{-\partial H}{\partial x_i};\ \lambda(1, t) = \frac{\partial G_1}{\partial x_i(1, t)} \quad i = 1, 2, \ldots r \qquad (18)$$

$$\frac{\partial \mu_j}{\partial t} = \frac{-\partial H}{\partial y_j};\ \mu_j(z, 1) = \frac{\partial G_2}{\partial y_j(z, 1)} \quad j = 1, 2, \ldots q \qquad (19)$$

for the case where $\mathbf{x}$ and $\mathbf{y}$ are unspecified at $z = 1$, $t = 1$, respectively. Also the discontinuities in the adjoint variable $\boldsymbol{\lambda}$ from bed to bed are given by

$$\lambda_j(\alpha_k^-, t) = \lambda_i(\alpha_k^+, t)\,\frac{\partial h_i}{\partial x_j(\alpha_k^-, t)} \qquad (20)$$

A second-order necessary condition is that the second variation $\delta^2 I$ be nonpositive for all small unconstrained variations. This reduces to $(\partial^2 H/\partial^2 \mathbf{u}_k)$ being negative semidefinite for optimal controls $\mathbf{u}_k(z, t)$. However, for $\mathbf{u}_k(t)$, $\mathbf{u}_k(z)$ there is no easy way to check the second-order condition, although the condition $(\partial^2 H/\partial \mathbf{u}_k^2)$ negative semidefinite is sufficient (not necessary) in this case. The proof of this theorem can be found in reference 5.

Although this maximum principle provides a basis for a large number of computational algorithms, we shall choose as in I to use a modified gradient method to correct an initial guess of the control. The computational algorithm is given in detail in I. The only modifications necessary for the multiple-bed case are inclusion of the spatial discontinuities in $\mathbf{x}$ and $\boldsymbol{\lambda}$ when integrating by the method of characteristics.

Through a slight modification of this maximum principle, the necessary conditions for reactors with interstage recycle (for example, part of the effluent from stage j is fed to stage k) can be obtained. However, since the computational algorithm for such systems is somewhat more involved, a subsequent paper will deal with recycle problems.

EXAMPLES

To illustrate the computational properties of this algorithm, a number of examples will be worked in detail. As in I, we shall assume there is but one catalyst activity whose decay is given by

$$\frac{\partial y_1}{\partial t} = -\rho \exp\left\{-\frac{1}{p\tau_k}\right\}(y_1)^2 = g_1 \quad \begin{matrix} 0 \leqq t \leqq 1 \\ 0 \leqq z \leqq 1 \end{matrix} \qquad (21)$$

where $0 \leqq w_1 \leqq 1$ is the initial catalyst activity in the beds, and τ_k is dimensionless reactor temperature in the k^{th} bed.

---

* The convention that a repeated subscript denotes a sum over that index is used throughout.

In solving the state and adjoint equations (by the method of characteristics) for these examples, the spatial direction was divided into three equal sections—$0 \leq z \leq 1/3$, $1/3 \leq z \leq 2/3$, $2/3 \leq z \leq 1$—usually with 16 mesh points in each section. In the temporal direction, normally 124 mesh points were used in the interval $0 \leq t \leq 0.25$ and another 124 in the remainder $0.25 \leq t \leq 1$.

We shall treat three separate kinetic schemes in both isothermal and adiabatic reactors as well as find the best catalyst loading and interstage feed distribution for the adiabatic reactor case.

ISOTHERMAL REACTORS

The optimal isothermal temperature for three beds with pure catalyst and no interstage feeds was determined for the following examples.

Irreversible First-Order Reaction ($A_1 \rightarrow A_2$)

For this case the state equations are

$$\frac{\partial x_1}{\partial z} = \beta_1 y_1 \exp\left(-\frac{1}{u_k}\right)(1 - x_1) = f_1 \qquad \begin{matrix} 0 \leq z \leq 1 \\ 0 \leq t \leq 1 \end{matrix} \tag{22}$$

$$\begin{aligned} x_1(0, t) &= 0 & k &= 1 \\ x_1(1/3^-, t) &= x_1(1/3^+, t) & k &= 2 \\ x_1(2/3^-, t) &= x_1(2/3^+, t) & k &= 3 \end{aligned}$$

where the control u_k is temperature in k^{th} bed and x_1 is the dimensionless extent of reaction. The objective is to maximize the total amount of A_2 produced subject to $u_k \leq 0.080$. Thus our objective functional is

$$I = \int_0^1 x_1(1, t)dt \tag{23}$$

and our control corrections are made in the direction

$$\delta u_k(t) = \epsilon \int_{\alpha_k}^{\alpha_{k+1}} \frac{\partial H}{\partial u_k} dz \qquad k = 1, 2, 3 \tag{24}$$

where

$$\alpha = \begin{bmatrix} 0 \\ 1/3 \\ 2/3 \\ 1 \end{bmatrix} \tag{25}$$

The results in Figure 2 for the parameters shown were found from two starting points $u_k(t) = 0.080$ and $u_k(t) = 0.075$. In each case the gradient method stopped at the policy shown and $\int_0^1 Hdz$ increased at each iteration. The value of the objective for this policy was $I = 0.8917$. By treating this example as a lumped-parameter problem (possible only for isothermal reactors), Crowe (2) was able to show that the policy shown in Figure 2 is a saddle point and not a maximum of the Hamiltonian. In addition, Crowe produced a purely bang-bang policy which gave an improved I over the results in Figure 2. Using this as another starting point for our gradient method, we found the policy shown in Figure 3 (with $I = 0.9004$). As can be seen the policy is composed of switching the temperature in each bed between upper and lower bounds with short constant conversion paths sometimes arising. Because our control is only a function of t, we cannot easily check the second variation condition $\delta^2 I \leq 0$ in this problem. Thus this result cannot be claimed an optimum, but it is where our gradient method stopped improving I.

Further examples of reversible exothermic reactions and consecutive reactions were also treated in isothermal reactors with very good results; see reference 5.

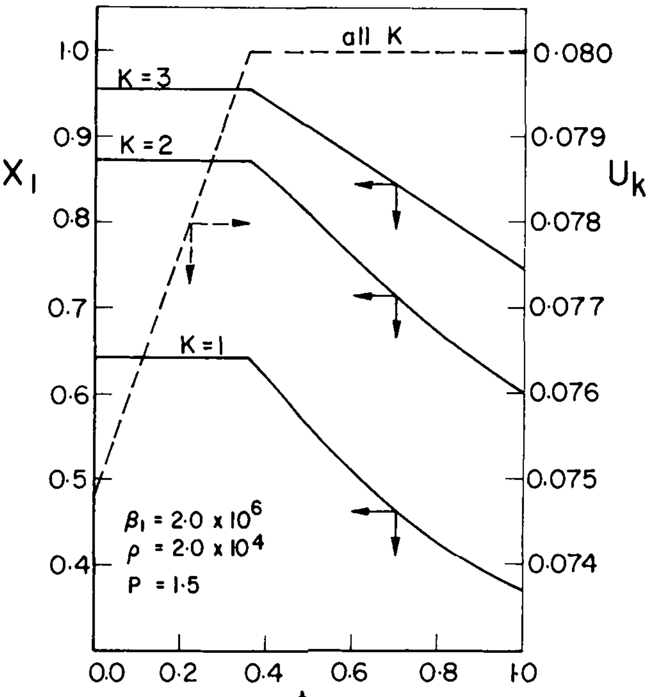

Fig. 2. First-order irreversible reaction example; isothermal reactors.

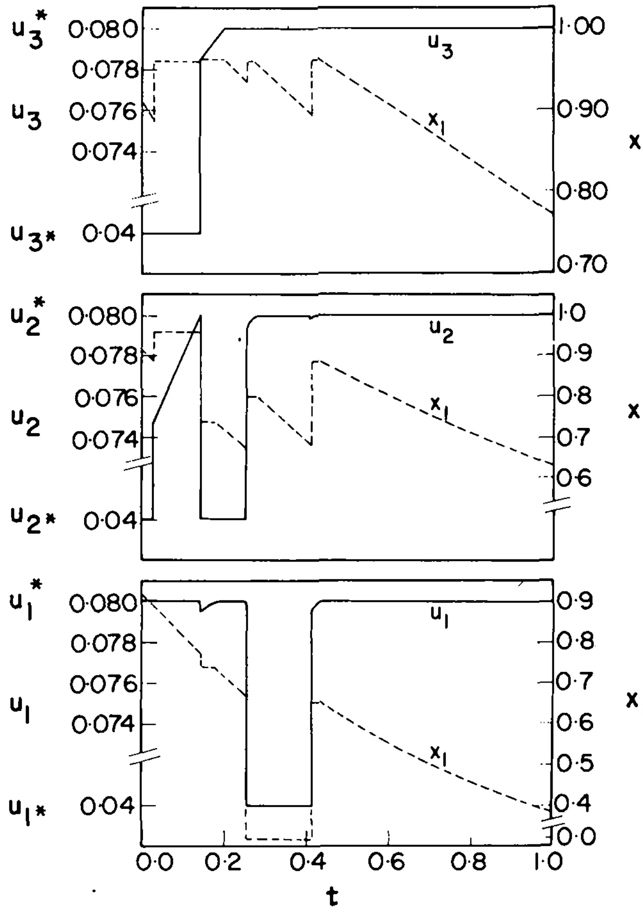

Fig. 3. First-order irreversible reaction example, isothermal reactors.

THE ADIABATIC REACTOR

As in I we will treat some examples of adiabatic reactor operation—this time in multiple beds. We recall that in the k^{th} bed the reaction temperature τ_k is related to the inlet temperature τ_{k0} and extent of reaction by

$$\tau_k = \tau_{k0} + \sum_{i=1}^{r} \left[J_i \{\xi_i(z,t) - \xi_i(\alpha_k{}^+, t)\}\right] \qquad k = 1, 2, \ldots N \tag{26}$$

so that we may exercise some control over reaction temperature by adjusting the inlet temperatures τ_{k0}. We shall now consider the same kinetic schemes as treated above to illustrate the optimal policy under adiabatic operation. The state equations are the same as above, except that reaction temperature is given by Equation (26) where τ_{k0} is our control variable u_k.

Irreversible First-Order Reaction ($A_1 \rightarrow A_2$)

The results for irreversible first-order endothermic reaction are given in Figure 4. The control policy shown was found in four ascents and 4 min. computing time* from two starting points, and constant conversion again appears to be the extremal policy in multiple-bed reactors for this case. When this result is compared with the same case in single beds, the multiple-bed reactor is found to have some advantage over a single bed. This is due to the better temperature control possible in multiple beds even when the inlet temperatures are the same as in Figure 4.

However, the previous isothermal reactor results led us to suspect that constant conversion might not be optimal even though it is an extremal policy. Thus a bang-bang starting point was used and the gradient method applied again with the result shown in Figure 5. The value of the yield for this policy is $I = 0.8969$, compared to the value $I = 0.8888$ for the constant conversion policy shown in Figure 4. This leads one to suspect that the policy shown in Figure 4 is a saddle point, whereas Figure 5 may be close to the optimum.

Reversible First-Order Reaction ($A_1 \rightleftarrows A_2$)

For this case the state equations become

$$\frac{\partial x_1}{\partial z} = y_1 \left[\beta_1 \exp\left(-u_k{}^{-1}\right)(1 - x_1) - \beta_2 \exp\left(-p_1 [u_k]^{-1}\right) x_1\right] = f_1 \tag{27}$$

with the discontinuity conditions given by Equation (22) and u_k given by Equation (26). The objective functional, steepest ascent direction, and bed lengths are given in Equations (23) to (25). The results for the first-order reversible exothermic reaction are given in Figure 6. The control policies were found after five ascents and 5 min. computing time from two different starting points, and show that the falling temperatures from bed to bed give about a 6% advantage over the optimum found in I for a single bed. This is due to the ability to approximate more closely the maximum reaction rate temperature in multiple beds.

Consecutive First-Order Reactions ($A_1 \rightarrow A_2 \rightarrow A_3$)

The state equations for this case are

$$\frac{\partial x_1}{\partial z} = \beta_1 y_1 \exp\left(-u_k{}^{-1}\right)(1 - x_1) = f_1 \tag{28}$$

$$\frac{\partial x_2}{\partial z} = \beta_2 y_1 \exp\left(-p_1 [u_k]^{-1}\right)(x_1 - x_2) = f_2 \tag{29}$$

with discontinuity equations in both x_1 and x_2 in the form of Equation (22) and u_k given by Equation (27). The objective remains the maximum production of A_2, but this now takes the mathematical form

$$I = \int_0^1 [x_1(1,t) - x_2(1,t)]dt \tag{30}$$

The results shown in Figure 7 were found in about six ascents and 5 min. computing time from two starting points. Since the objective functional is essentially the same as for the single-bed problem solved in I, at first there appeared to be no great advantage to multiple beds in this case. However, this result is due to the fact that

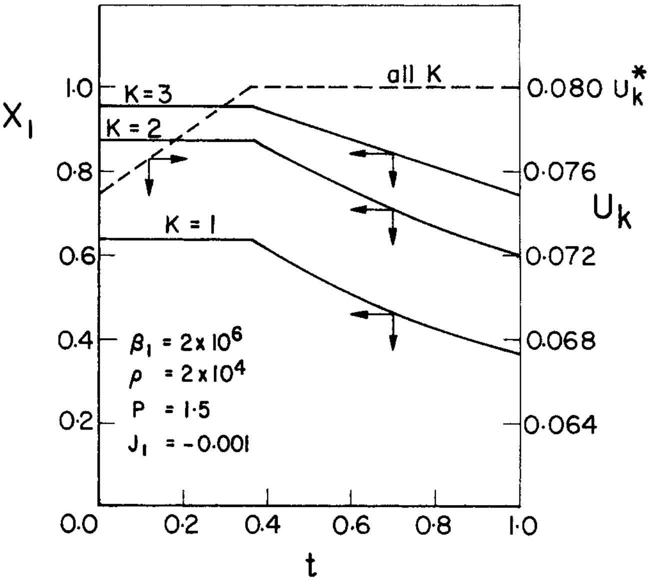

Fig. 4. First-order irreversible endothermic reaction example; adiabatic reactors.

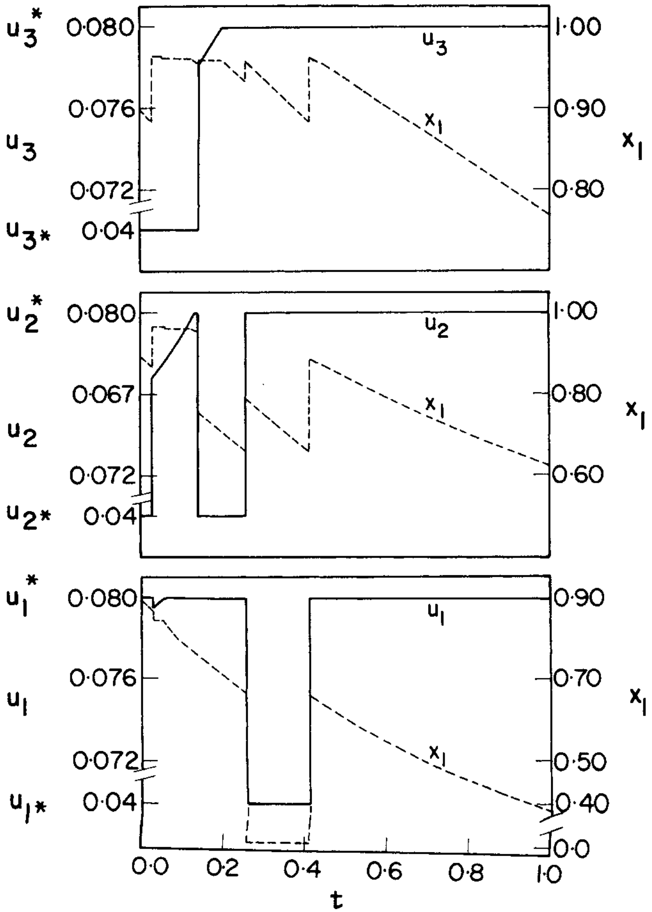

Fig. 5. First-order irreversible endothermic reaction example; adiabatic reactors.

---

* All computing times quoted are for an IBM 360/75.

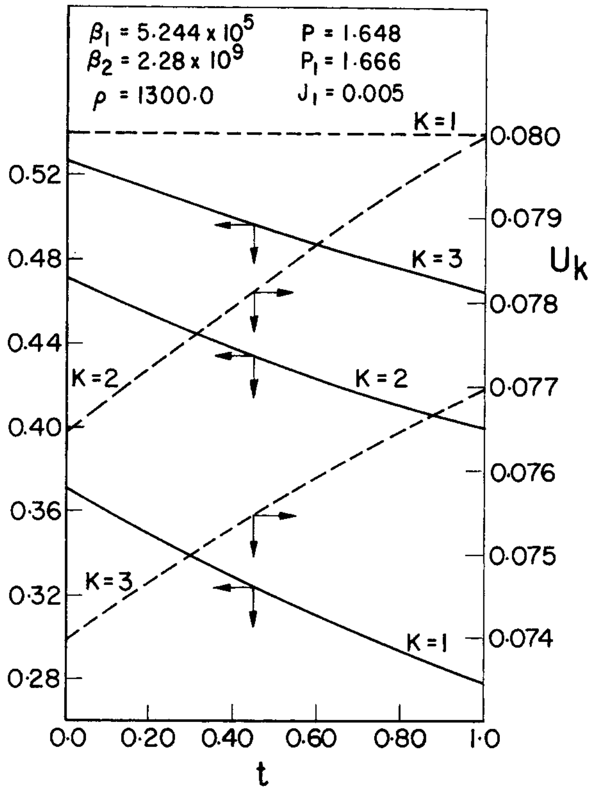

ig. 6. First-order reversible exothermic reaction example; adiabatic reactors.

alling temperature profile in the single-bed reactor is almost identical to the optimum multiple-bed profile for this particular set of kinetic parameters. In general, multiple beds should have advantages over single beds for this system.

A FEED ALLOCATION PROBLEM

In order to illustrate the algorithm when it is desired to allocate feed optimally between beds, we will find the optimal adiabatic temperature policy, the optimal feed distribution, and optimal residence time in each bed simultaneously using our algorithm. Suppose we have the well-known reaction $A_1 \rightleftarrows A_2$ taking place in three beds. We think that we may be able to operate to some advantage by splitting our feed A_1 between the three beds and varying the total residence time over the lifetime of operation.

Our objective functional for this problem is

$$I = \int_0^1 \left\{ \left[\sum_{k=1}^{3} \eta_k \right] [x_1(1,t) - C_1[1 - x_1(1,t) - C_3 x_1(1,t)] \right\} dt \qquad (31)$$

where the first term represents the value of A_2 produced, the second term the cost of separating A_1 from the product stream, and the last term is the cost of reactant A_1 consumed. The quantity

$$\eta_k = \sum_{i=1}^{r} q_{ik} \quad k = 1, 2, \ldots. N \qquad (32)$$

is the total flow rate of feed to stage k, and for this example is composed entirely of A_1.

The state equation for this problem becomes

$$\frac{\partial x_1}{\partial z} = y_1[\hat{\beta}_1 \exp\{-(u_k + J_1[x_1(z,t) - x_1(\alpha_k{}^+, t)])^{-1}\}(1 - x_1) - \hat{\beta}_2 \exp\{-p_1(u_k + J_1[x_1(z,t) - x(\alpha_k{}^+, t)])^{-1}\} x_1] \left\{ \sum_{j=1}^{k} \eta_j \right\}^{-1} \qquad (33)$$

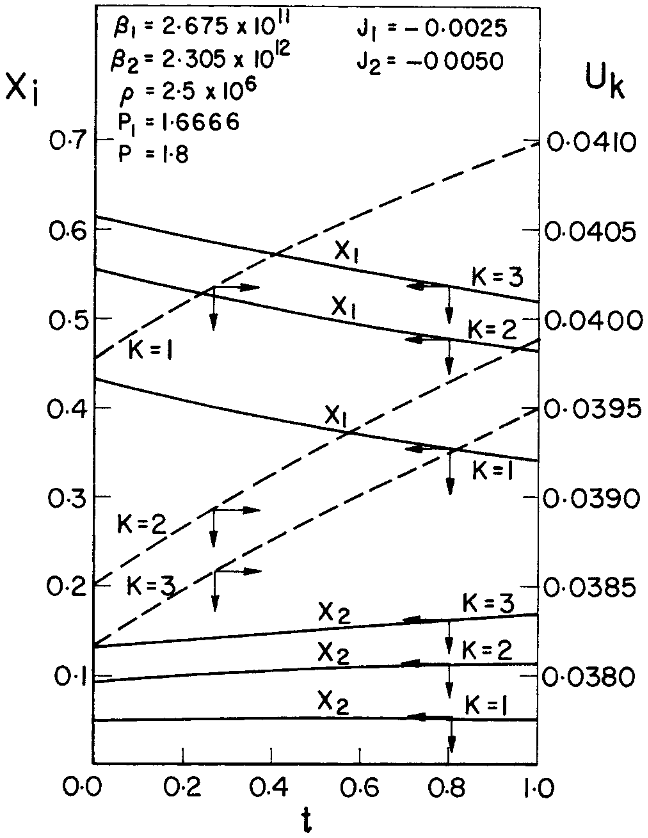

Fig. 7. Consecutive first-order reaction example; adiabatic reactors.

with the linear blending condition at each bed

$$x_1(\alpha_k{}^+ \ t) = \frac{\left[\sum_{j=0}^{k-1} \eta_j \right] x_1(\alpha_k{}^-, t)}{\left[\sum_{j=1}^{k} \eta_j \right]} \qquad (34)$$

where $\eta_0 = 0$. In this example $\hat{\beta}_1$, $\hat{\beta}_2$ are defined so that the spatial direction is a dimensionless reactor volume. Thus if we pick three beds of equal volume, then the discontinuity vector $\boldsymbol{\alpha}$ is given by Equation (25).

If we solve the control problem with only the constraints $\eta_k \geqq 0$ on the feed control vector, we will automatically get the optimal residence time in each bed from the algorithm.

Using our modified gradient method and making our corrections in η_k at each ascent in the direction

$$\delta\eta_k = \epsilon \frac{\partial H_1}{\partial \eta_k} \qquad (35)$$

we obtained the results shown in Figure 8 for $C_1 = 0.25$, $C_3 = 0.40$. The policy shown was obtained from two different starting points in about ten ascents and 7 min. computing time. These results, when compared with the optimal policy (at the same total throughput) for a single-bed reactor of the same total volume but with constant flow rate, showed a 28% improvement in the objective. A similar comparison with an optimal constant flow rate, three-

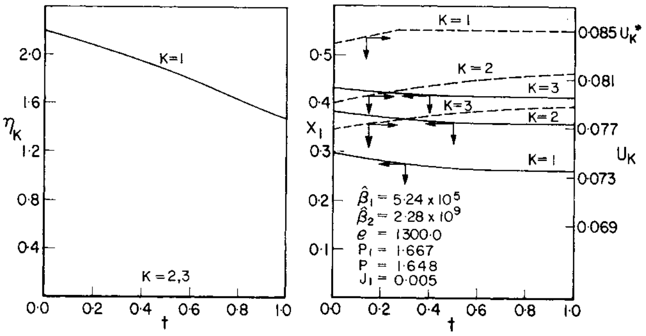

Fig. 8. Adiabatic temperature policies with interstage feed distribution.

bed reactor showed that varying the flow rate optimally produces about 1% improvement in the profit. It is interesting that the optimal policy is to decrease throughput as the catalyst decays to maintain the conversion from the reactor essentially constant, a common industrial practice.

THE COMPLETE PROBLEM

Let us now consider the previous example but with the additional complication that catalyst is expensive (with cost a) and the loading must be picked optimally. In this case the objective functional is given by

$$I = \int_0^1 \left\{ \left[\sum_{k=1}^{3} \eta_k \right] [x_1(1,t) - C_1 [1 - x_1(1,t)] - C_3 x_1(1,t)] \right\} dt - a \int_0^1 w_1(z,0) dz \quad (36)$$

From Equations (16) and (17) it is seen that for beds in which

$$a \leqq \mu_1(z,0) \quad (37)$$

[where $\mu_1(z,0)$ are the values from the previous pure catalyst example], pure catalyst is the optimal loading. In the previous case it was found that

$$\min_{z} \{\mu_1(z,0)\} = 0.105 \quad (38)$$

so that for $a \leqq 0.105$ pure catalyst is the optimal policy in each bed. The optimal policy for $a = 0.15$ was sought from two different starting points and the points where the gradient method stopped are shown in Figures 9 and 10. Even though the temperature controls and state variables are nearly identical for the two policies shown, the differences in the flow rate and catalyst loading controls produce a difference in the objective of about 2%. The optimum is probably somewhere between the two policies shown.

The convergence difficulties here are probably due to the singular nature of the flow rate and catalyst loading control policies, which are known to be resistant to gradient methods. The computing times, however, were still very modest, for example, policy *A* required only eight ascents and 7 min. computing effort.

CONCLUSIONS

We have extended the theory for single beds developed in I to multiple-bed reactors suffering catalyst decay. In addition we have illustrated in great detail how the optimal policies can be synthesized for a number of examples. The good convergence of gradient methods for such systems is quite remarkable, particularly in the cases where optimal catalyst loadings and feed distributions were found, because these policies are singular ones for which solution by gradient methods is usually very difficult (*4*). Since all of our examples showed reasonably good convergence, it is impossible to say with certainty whether this very desirable property will carry over to more complex problems. However, the fact that we have been able to find saddle points (Figures 2 and 3) by climbing with our gradient method should make one cautious in proclaiming a numerically determined policy optimal. Nevertheless, the theory presented is an adequate and useful framework to study multiple-bed catalyst decay problems, and the computational algorithm is adequate for improving existing operating policies.

Since many reactors subject to catalyst decay are operated in a cyclic fashion—with one or more reactors being regenerated while others are operating—work is in progress to study the optimal control of such reactors. This mode of operation is particularly appealing for irreversible reactions for $p > 1$ in light of the optimal policies shown in Figures 3 and 5. These indicate natural periods of no throughput for each reactor and if these periods of time were used for catalyst regeneration, then the optimums shown could certainly be improved.

ACKNOWLEDGMENT

We thank the National Research Council of Canada for supporting this work through Grant A-3859. In addition, we are indebted to the University of Waterloo Computing Centre for furnishing computing time for the study.

NOTATION

a = average cost of catalyst over the lifetime of operation

A_0 = pre-exponential factor for fouling reaction rate

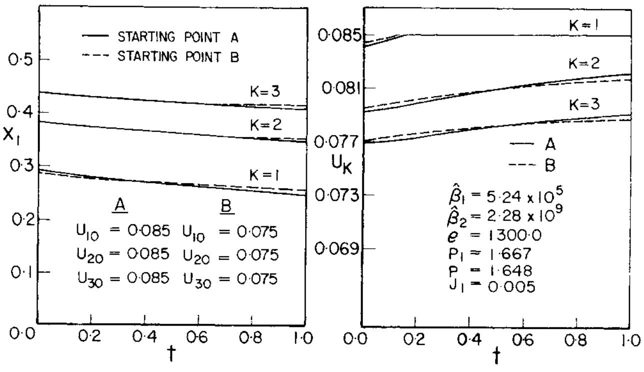

Fig. 9. The complete problem.

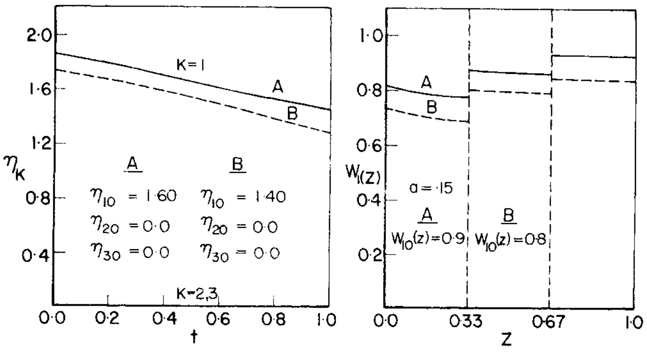

Fig. 10. The complete problem.

constants
A_{i0} = pre-exponential factors of main reaction rate constant
C_p = specific heat of reaction mixture
C_1 = cost of separation of reactant from product
C_2 = cost of separation of byproduct from product
C_3 = cost of reactant
E = activation energy of fouling reaction rate constant
E_i = activation energies of main reaction rate constants
f_i' = rate of the i^{th} chemical reaction
G, G_1, G_2 = integrands of objective functional
g_k' = rate of the k^{th} fouling reaction
H, H_1, H_2 = Hamiltonians
ΔH_i = heat of reaction of the i^{th} chemical reaction
h_i = blending function
I = objective functional
$J_i = \left(\frac{-\Delta H_i}{C_p}\right)\left(\frac{R}{E_1}\right)$
L' = total reactor residence time
P = pressure
$p = E_1/E$
$p_1 = E_2/E_1$
q_0' = reference feed rate
$\mathbf{q}_k'$ = feed rate vector to k^{th} bed
$\mathbf{q}_k$ = dimensionless feed rate vector to k^{th} bed $= \mathbf{q}_k'/q_0'$
T = temperature
t' = time
$t = t'/\theta$
$\mathbf{u}_k$ = control variable vector in the k^{th} bed
V = total reactor volume
$w(z)$ = initial catalyst activity along the reactor length
$\mathbf{x}, \mathbf{y}$ = state variables
z' = residence time in the reactor
z = dimensionless spatial coordinate

Greek Letters

α_k^- = spatial coordinate of end of $(k-1)^{\text{st}}$ bed
α_k^+ = spatial coordinate at beginning of k^{th} bed
$\beta_1 = A_{10} \cdot L$
$\beta_2 = A_{20} \cdot L$
$\hat{\beta}_1 = A_{10}V/q_0'$
$\hat{\beta}_2 = A_{20}V/q_0'$
ϵ = scalar constant
θ = total on-stream time
$\lambda_i \mu_i$ = adjoint variables
ξ_i = extent of the i^{th} reaction, or concentration of i^{th} species
$\rho = A_0\theta$
$\tau = RT/E_1$
Ψ_k = instantaneous catalyst activity for the k^{th} catalytic agent

LITERATURE CITED

1. Ogunye, A. F., and W. H. Ray, *AIChE J.*, 17, 43 (1971).
2. Crowe, C. M., paper presented at AIChE Washington Meeting (Nov. 1969).
3. Aris, Rutherford, "Elementary Chemical Reactor Analysis," p. 65, Prentice-Hall, Englewood Cliffs, N. J. (1968).
4. Johansen, D. E., "Advan. Control Systems," 4, 279 (1966).
5. Ogunye, A. F., Ph.D. thesis, Univ. Waterloo, Canada (1969).

Manuscript received August 20, 1969; revision received January 1, 1970; paper accepted January 19, 1970.

Diffusion and Reaction in Ideal Multicomponent Systems:

I. Tubular Reactor near Equilibrium

R. L. SOLOMON and J. L. HUDSON
University of Illinois, Urbana, Illinois

Diffusion and either surface or gas-phase reaction in a ternary ideal gas mixture in steady fully developed laminar flow in a tube is considered. The linearized equations valid near equilibrium and under isothermal conditions are solved. Concentration profiles predicted using a multicomponent diffusivity matrix are compared to those predicted using more approximate diffusivities. Local overshoots past equilibrium occur, but oscillations (with axial position) are not possible. A simplified diffusivity expression is found which predicts cup-mixing mole fractions in good agreement with those predicted using the multicomponent diffusivities.

In a multicomponent mixture the diffusional flux of each component depends on the spatial variation of the concentration of all the species. If the fluxes depend linearly on the mole fraction gradients according to an expression of the form

$$J_i^* = -c \sum_{j=1}^{N} D_{ij}^* \nabla x_j \tag{1}$$

and if no chemical reaction occurs, the species mass balances can be uncoupled; the solutions of the equations governing the multicomponent system can then be found in terms of solutions of analogous binary problems (*6, 7, 27, 29, 30*).

If a chemical reaction occurs the species mass balances can not, in general, be uncoupled (*31*). Interesting and important effects due to the coupling in diffusion and reaction can occur in multicomponent systems. Toor (*31*) considered transient diffusion and gas-phase reaction in a one-dimensional nonflow multicomponent system. The linearized equations were solved by separation of variables. Toor showed that the eigenvalues for an ideal system near

---

R. L. Solomon is at Manchester University, Manchester, England.